THE JOURNAL OF PHYSICAL CHEMISTRY B

Article

Cite This: J. Phys. Chem. B XXXX, XXX, XXX−XXX

pubs.acs.org/JPCB

Evolved Minimal Frustration in Multifunctional Biomolecules

Konstantin Röder and David J. Wales*

Department of Chemistry, University of Cambridge, Lensfield Road, Cambridge, CB2 1EW, U.K.

Supporting Information

ABSTRACT: Protein folding is often viewed in terms of a funneled potential or free energy landscape. A variety of experiments now indicate the existence of multifunnel landscapes, associated with multifunctional biomolecules. Here, we present evidence that these systems have evolved to exhibit the minimal number of funnels required to fulfill their cellular functions, suggesting an extension to the principle of minimum frustration. We find that minimal disruptive mutations result in additional funnels, and the associated structural ensembles become more diverse. The same trends are observed in an atomic cluster. These observations suggest guidelines for rational design of engineered multifunctional biomolecules.

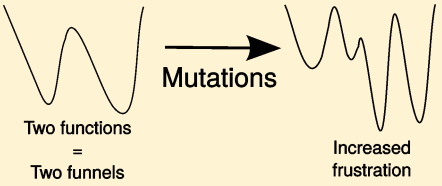

INTRODUCTION

The structure−function paradigm is the cornerstone of our understanding for biological processes at a molecular level. If it is possible to identify the populated structural ensembles, and the interconversion pathways between these ensembles, a mechanistic interpretation of functionality is possible. Understanding how biomolecules achieve their functional state is therefore a key research goal. One theoretical framework to address this problem is provided by the potential energy landscape, which contains all of the information necessary to understand the molecular thermodynamic, kinetic, and structural properties.

A central paradigm in explaining the organization of energy landscapes is the principle of minimal frustration;[1−7] here, frustration is defined in terms of competing low-energy minima separated by high barriers. Functional globular proteins appear to have evolved to reduce frustration as far as possible, and usually exhibit single-funneled landscapes based on a particular global minimum structural ensemble. In this case, a single funnel on the potential energy landscape can be used to define a single funnel on the free energy landscape for physiological temperatures of interest. Nelson and Onuchic[8] showed that minimal frustration in natural proteins leads to sequences that have evolved to support the native contacts in the global minimum structural ensemble, resulting in a deep funnel.

The functional structure is still likely to be recognizable for mutations corresponding to minimal perturbations, even though these changes may increase frustration. The evolution of amino acid sequences is therefore influenced by selection pressures determining stability, accessibility, and function.[9] Indeed, there is both theoretical and experimental evidence that maintaining the structure of the native fold is an important constraint on evolution.[7] This optimization, leading to tolerance of sequence modification, may also play a role in the success of Φ-value analysis[10,11] for conservative mutations, which can be treated from a perturbative viewpoint.

More generally, single-funneled potential energy landscapes have been associated with self-organization or "structure-seeking" properties throughout molecular science and for condensed and soft matter.[12,13] These properties have been illustrated and analyzed for a diverse range of systems, including "magic number" atomic and molecular clusters, crystals, and self-assembling mesoscopic structures, such as shells and helices.

While analysis of single-funneled potential energy landscapes has provided detailed explanations for self-organizing capabilities, which resolve the Levinthal paradox, an increasing number of studies describe multifunneled protein energy landscapes.[14−16] It seems reasonable that a system will have to adopt more than one distinct configuration to encode more than one function, with the relative stabilities potentially tunable by environmental conditions, or binding of specific partner ligands, which might relieve the residual frustration associated with alternative structures.[17] The system can then switch between states to regulate functionality. Double-funnel landscapes have also been associated with open and closed forms of enzymes such as adenylate kinase.[18] It seems unlikely that two distinct functional morphologies would be optimized within a single potential energy funnel, necessitating the evolution or design of multifunneled landscapes.

In the present work, we suggest that multifunctional biomolecules have evolved to minimize frustration in their multifunneled energy landscapes. We present evidence that proteins and nucleic acids support the minimum number of funnels necessary to fulfill their function. In particular, we show that minimal disruptive mutations change the potential energy landscape, producing additional funnels and more diverse structural ensembles. Here we define a minimal disruptive mutation as one that shifts the equilibrium populations of the competing morphologies, while retaining recognizable funnels corresponding to the unperturbed system on the transformed

Special Issue: William A. Eaton Festschrift

Received: April 17, 2018
Published: May 25, 2018

DOI: 10.1021/acs.jpcb.8b03632
J. Phys. Chem. B XXXX, XXX, XXX−XXX

landscape. For such perturbations, we identify two key results: (a) increased frustration as a result of additional funnels and larger energy barriers and (b) greater structural diversity in the funnels on the perturbed landscapes, due to weakening of native contacts. Further tests for a double-funnel atomic cluster reproduce both trends, as illustrated in the Supporting Information. Our calculations are based on the computational potential energy landscape framework, which is founded on geometry optimization with postprocessing using the tools of statistical mechanics and unimolecular rate theory to predict structure, dynamics, and thermodynamics.

METHODS

The Computational Potential Energy Framework. Potential energy landscapes were explored using discrete path sampling[19,20] to construct kinetic transition networks,[21,22] which consist of local minima and the transition states that connect them. The doubly-nudged elastic band algorithm[23−25] coupled with hybrid eigenvector-following[26] was used to locate transition states. The minima connected by the transition states were then characterized using approximate steepest-decent pathways. Further details are available in several reviews.[16,22]

Starting Configurations and Force Field Settings. We employed the AMBER ff14SB[27] force field. To reduce the computational cost, implicit generalized Born solvation[28,29] models were used without cutoffs, together with the Debye−Hückel approximation[30] for ions (0.1 M). The starting points for path sampling for the coiled-coil, ubiquitin, and RNA 7SK were crystal structures taken from experimental work, as indicated below. For oxytocin and vasopressin, we used basin-hopping global optimization[31−33] to locate low-energy structures.

Visualization and Frustration. The global organization of an energy landscape is best visualized using disconnectivity graphs,[13,34] and we couple these illustrations with a numerical index[35] to quantify the frustration associated with the increased number of funnels and higher barriers. The greater heterogeneity in the residual native funnels after mutation is manifested in terms of increased structural diversity, and in the distribution of secondary structural elements.

RESULTS

A Coiled-Coil Conformational Switch. The first example considered here is a coiled-coil molecular switch between parallel and antiparallel helical alignments.[36,37] The coiled-coil arrangement, a common motif for peptides, formed by the association of multiple supercoiled α-helices, provides an important test case for protein folding, together with an attractive starting point for protein design,[38] and has been the subject of several computational studies.[39,40]

The most important structural feature exhibited by coiled-coils is the hydrophobic core formed between the helices. A well-studied system is the leucine zipper of the yeast transcription factor GCN4[41] and the family of coiled-coils derived from it.[42] This family exhibits interesting assembly properties. Depending on the solvent and the precise sequence, multiple oligomer sizes for the coiled-coil have been characterized.[43] Competition has also been observed between parallel and antiparallel alignment of the α-helices,[38] which is probably encoded via a multifunnel energy landscape. A multifunnel landscape was predicted for a similar system, namely the Rop dimer,[44] and later experimentally confirmed.[45] In this case, mutations may switch the stabilities of competing topologies, producing apparently anomalous kinetic effects.

In the example of GCN4-pLI, the native sequence only exhibits the parallel structure.[36] A single point mutation, E20S, stabilizes both antiparallel and parallel arrangements. The energy landscapes for both cases are shown in Figure 1,

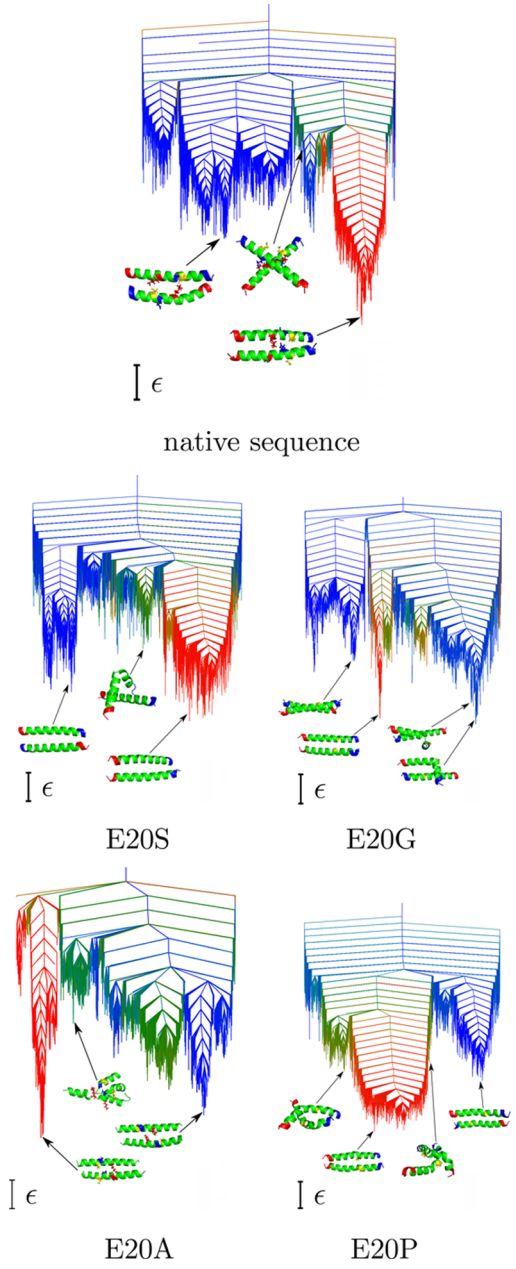

Figure 1. Top: Disconnectivity graphs for the native sequence (left) and E20S mutant (right) of GCN4-pLI with representative structures for all funnels, highlighting the change in relative energies. An additional funnel corresponding to intermediate structures appears for the E20S mutant. The coloring is defined by an order parameter q, which identifies the angle between the two helices, ranging from 0 (red, parallel) to 1 (blue, antiparallel). Bottom: Disconnectivity graphs for the E20G, E20A, and E20P mutants. Although the two distinct funnels for parallel and antiparallel configurations are preserved, additional funnels appear for E20G and E20A, which increase the frustration and disorder. For the E20P mutant, the funnel corresponding to parallel structures exhibits greater structural diversity. ϵ is 8 kcal mol^{-1}. Adapted from previous work.[37]

DOI: 10.1021/acs.jpcb.8b03632
J. Phys. Chem. B XXXX, XXX, XXX−XXX

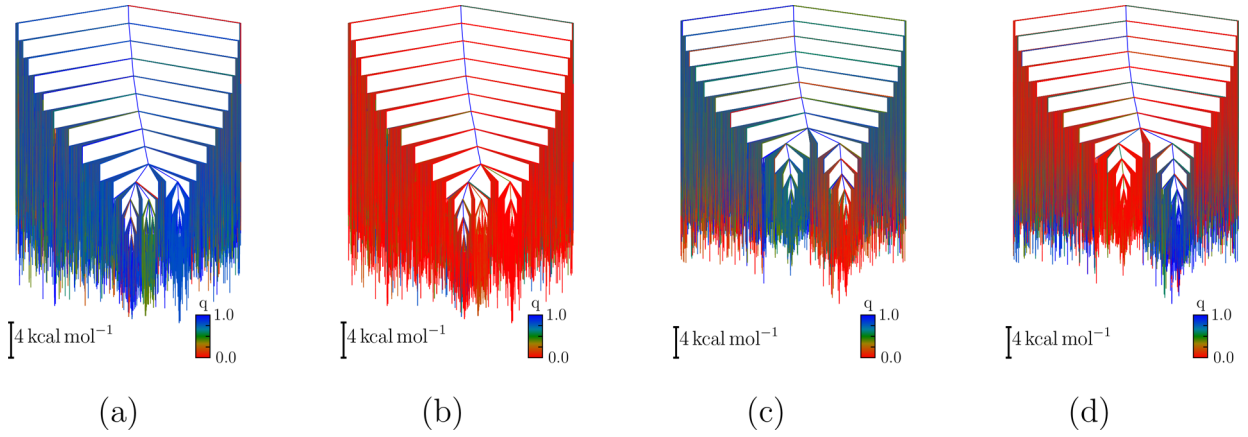

Figure 2. Disconnectivity graphs (a and b) for wild type oxytocin and (c and d) for the Q4T+P7G mutant. The colors correspond to distinct structural elements: parts a and c highlight bends, and parts b and d highlight turns, where blue means that the motif is present and red that it is absent. The mutant exhibits greater structural diversity.

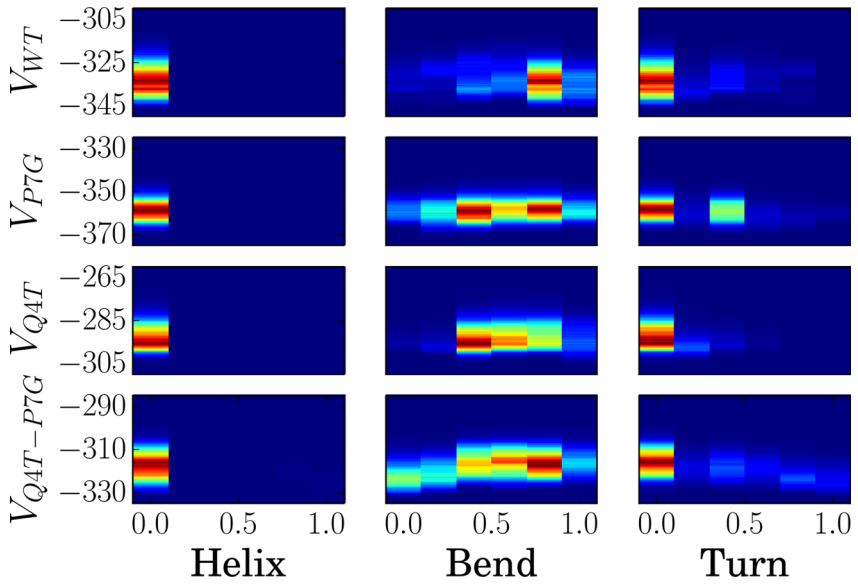

Figure 3. 2D heatmaps showing the proportion of residues in a helical configuration, a bend, or a turn, as a function of the potential energy (in kcal mol^{-1}) for oxytocin where red indicates a large number of structures, and dark blue an absence of structures in this configuration. The mutations are indicated in the subscripts. Comparing the wild type (top row) to the mutants, the structural diversity increases significantly.

together with representative structures associated with the alternative funnels. In the native sequence, the antiparallel configurations are suppressed by a high energy barrier between the funnels and a salt bridge formed with residue 20. Removing this key interaction and replacing it with a weaker, but still polar, interaction in the E20S mutant lowers the energy of the antiparallel funnel and destabilizes the parallel alignment, enabling two competing structural ensembles to be observed,[37] along with a low energy intermediate.

The frustration index[35] for the native sequence is an order of magnitude lower than for the E20S mutant. For a set of more disruptive mutations, namely, E20A, E20G, and E20P (shown in Figure 1), further changes to the landscape are observed. While the two key structural motifs are still preserved, a number of additional low energy funnels appear for E20A and E20G. The increase in frustration leads to complexity reminiscent of the landscapes recently characterized for intrinsically disordered peptides.[5,46,47] For the E20P mutation, the width of the funnels increases, because nonspecificity in the interactions allows for more structural variety, destabilizing both parallel and antiparallel alignments. Here, the increased funnel width means that a larger number of structures have relatively low energy, because there is a loss of specificity in the stabilizing interactions. While small changes, such as the E20S mutation, may lead to potentially useful two-state systems and switches, the disruptive mutations produce a more diverse set of structures, where control of functionality is likely to be difficult.

Oxytocin and Vasopressin. Competing structural ensembles have been reported for oxytocin and vasopressin,[48] and both hormones have been characterized as disordered.[48] The key structural motif of these nonapeptides is a disulfide bond between cysteine residues in positions 1 and 6, forming a ring of six amino acids and a three-membered tail. The activities of both hormones, and indeed the binding to transport proteins, is drastically reduced by mutations.[49−51] These experimentally observed alterations in binding affinities make the hormones interesting targets to better understand biospecificity, in particular with respect to point mutations. We explored the energy landscape for oxytocin and its Q4T, P7G, and Q4T

DOI: 10.1021/acs.jpcb.8b03632
J. Phys. Chem. B XXXX, XXX, XXX−XXX

+P7G mutants and for vasopressin and its P7L and Y2H mutants, in the absence of binding partners, as in previous work.[48] Vasopressin and oxytocin are themselves related by a pair of mutations (I3F and L8R). All of these mutations change the number of distinguishable funnels on the energy landscape, as revealed in the corresponding disconnectivity graphs (Figure 2). Heatmaps of the propensity for different secondary structures in the core region of the peptide (residues 3−7) as a function of the potential energy are shown in Figure 3. The analogous plot for vasopressin is provided in the Supporting Information. Increased structural diversity is also observed in the radius of gyration.[48] These shifts in population between different structures move the systems away from the conformations adopted for binding to various carriers and acceptors[48] and increase the disorder, which is again reflected in the frustration indices.

Ubiquitin. Our third example is ubiquitin, a signaling protein. Recently, it was shown that ubiquitin exhibits two distinct conformations, Ub and Ub-CR.[52] In the newly described Ub-CR conformation, the C-terminal tail is retracted. The recent finding of a second "hidden" conformation of ubiquitin is of great biological importance. Although relatively unpopulated, the Ub-CR conformation is the target of phosphorylation by PINK1,[53] and a perturbation of this event leads to hereditary forms of Parkinson's disease.[54] Interestingly, the resulting phosphorylated ubiquitin also exhibits a higher propensity for the Ub-CR conformation.[55,56] Modulation of the equilibrium between the two states therefore regulates the activity of ubiquitin.

The introduction of a single mutation, L67S, shifts the equilibrium toward the Ub-CR conformation.[52] Figure 4 shows disconnectivity graphs for the wild type (native state) and the L67S mutant. For the wild type, we find two distinct funnels. However, the higher energy feature has less than 1% occupation probability at physiological temperatures, consistent with experiment and with the successful prediction of hydrogen exchange rates using a single funnel model.[57] For the mutant, not only are the relative energies of the funnels shifted, but the energy barriers between the smaller subfunnels are larger, and hence become relevant for the conformational dynamics. The mutation produces greater frustration compared to the wild type, which exhibits only the two funnels necessary to stabilize the two biologically functional configurations. The corresponding frustration index is again roughly an order of magnitude lower in the wild type.

The HP1 Hairpin of RNA 7SK. Finally, we summarize results for the HP1 hairpin of RNA 7SK. RNA 7SK is involved in regulating the transcription pausing of RNA-polymerase II[58,59] and can be indirectly linked to the transcription of HIV RNA.[60] Transcription involves binding to the HEXIM protein[61,62] through the 5′-hairpin of 7SK (HP1). Recent experiments have shown that the binding involves specific triplet patterns formed by unpaired bases, and mutations perturb this pattern, leading to a loss of binding affinity.[63] In the wild type sequence, the energy landscape is clearly partitioned into three funnels, two of which correspond to the states identified in crystal structures.[63] The third funnel is an artifact of the HP1 model: the RNA hairpin is truncated to reduce the computational cost and can therefore bend back onto itself. Aside from this artifact, the landscape consists of two funnels corresponding to the two distinct states observed in nature. For a range of mutations, the frustration increases, due to additional distinct subclasses of conformations separated by high energy barriers. Two examples are shown in Figure 5.

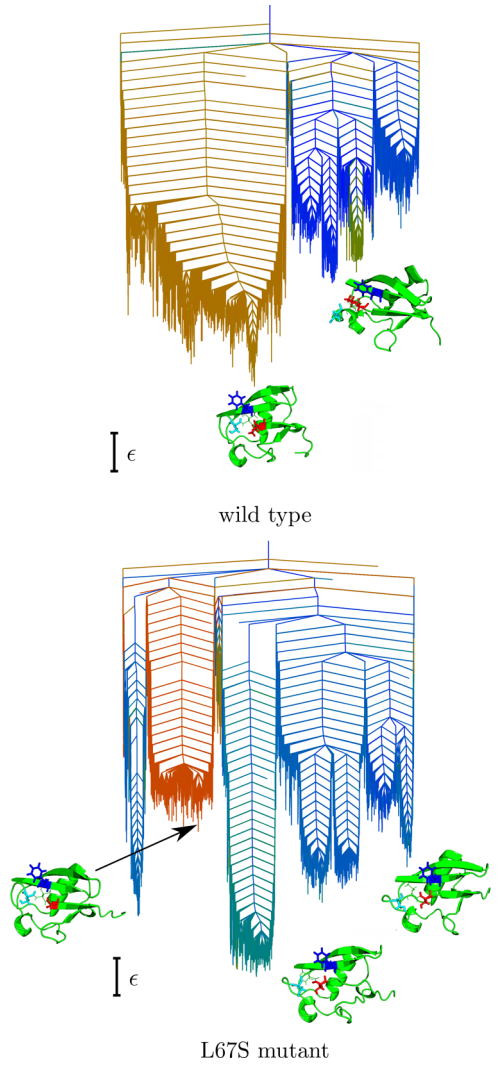

Figure 4. Disconnectivity graphs for the potential energy landscapes of the wild type (left) and L67S mutants (right) of ubiquitin. r is the normalized ratio of the distances between the Cα atoms of residues 4 (blue) and 65 (cyan) and residues 4 and residue 67 (red). The Ub-CR configurations have a large r value (blue in the disconnectivity graph), while the Ub configurations have small values (red and orange). Increased frustration and disorder is evident for the mutant. ϵ is 8 kcal mol^{-1}.

CONCLUSION

In summary, we have presented evidence that some specific biomolecules have evolved to exhibit the minimal number of funnels on their energy landscape to fulfill their functions. While the structure of a single-funneled energy landscape resolves the Levinthal paradox,[64,65] and many examples have been analyzed throughout molecular science, multifunnel landscapes also exist. We suggest that these landscapes have evolved to reduce frustration by supporting the minimal number of funnels compatible with the required functionality.

Compared to the mutants we have considered, the landscapes for native sequences seem to be steeper and better optimized with respect to the lowest energy configuration, in agreement with the principle of minimal frustration;[1−7] i.e., the specificity of native interactions is highest for this sequence.

DOI: 10.1021/acs.jpcb.8b03632
J. Phys. Chem. B XXXX, XXX, XXX−XXX

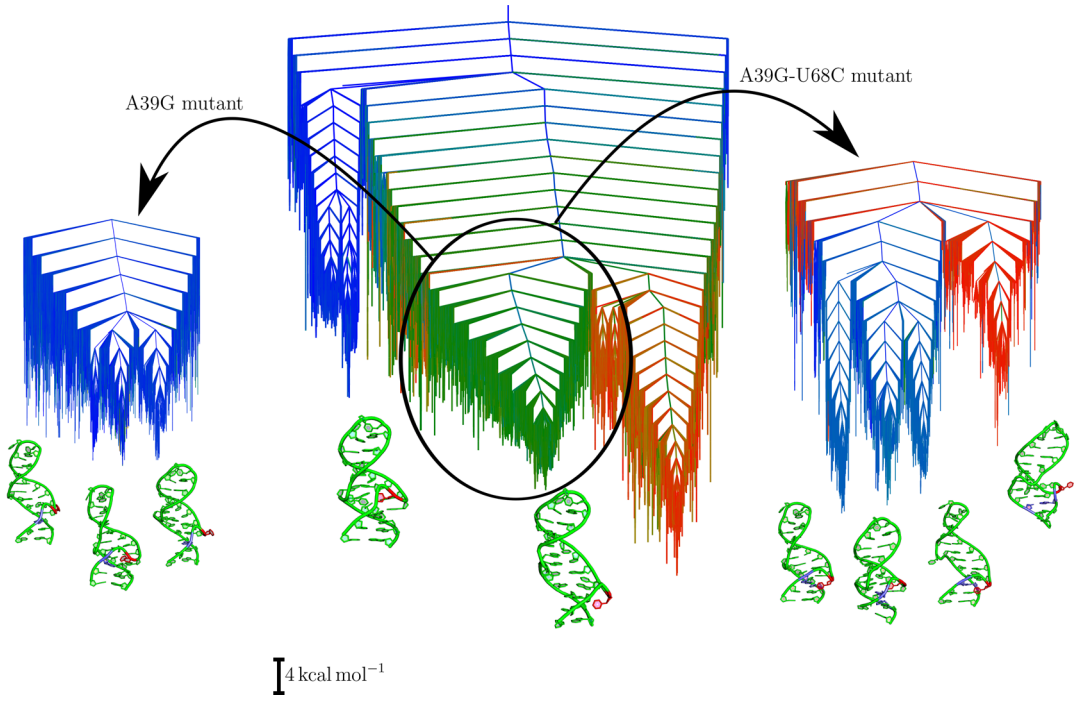

Figure 5. Disconnectivity graphs for RNA 7SK HP1. The disconnectivity graph for the native sequence is shown in the middle. The landscape exhibits three funnels; the one in red is an artifact of the hairpin truncation, consisting of structures that bend back on themselves. Aside from this artifact, the other two funnels (blue and green) correspond to the experimentally observed structures, with two distinct triplets forming inside the hairpin, leading to extended or shortened morphologies. Experiment indicates that these structures fulfill distinct functions, and consequently must correspond to distinct, switchable states. Upon mutation (left and right disconnectivity graphs), the extended funnel splits into multiple smaller funnels with distinct conformations, all based on the extended triplet morphology. The coloring is based on the positions of U40 and U41, which experiment indicates are involved in binding.

This effect also leads to greater structural variety within distinguishable conformational ensembles for the mutants, as illustrated for the E20P coiled-coil mutant and for oxytocin.

Point mutations may lead to additional funnels corresponding to alternative competing structural ensembles. The additional frustration increases disorder, which shifts the landscape from a well-defined multifunnel topography. In artificially engineered sequences, this effect is likely to produce a highly frustrated landscape, lacking well-defined functionality. New design principles should therefore focus not only on the desired functionality but also on minimizing frustration within a multifunnel scenario.

We also find that mutations generally introduce additional stable intermediates, which may lead to alternative reaction pathways. Such changes may be associated with misfunction and disease, since they introduce additional stable structures and kinetic traps, which might be exploited as experimental probes, providing access to configurational changes and intermediates. Some landscapes may be optimized for particular environments, including binding partners, and different environments could produce changes similar to those observed for minimal mutations. The multifunnel landscapes associated with intrinsically disordered proteins[47] may provide an example of this effect.

To further explore whether the observed trends apply beyond the realm of biomolecules, we have investigated the effect of analogous perturbations for an atomic cluster. In previous work, additional low temperature heat capacity features were observed in doped clusters,[66] resulting from alternative competing structures. To visualize the effect of such changes on the landscape, we considered an alchemical transformation for one of the core atoms in a double-funnel system, as detailed in the Supporting Information. As the magnitude of the perturbation increases, a new funnel with additional substructure appears, and the two original low-energy morphologies are shifted up the landscape. These results again suggest that weakening specific interactions, which stabilize key structures, will generally lead to additional low-energy morphologies and more diverse structural ensembles.

■ ASSOCIATED CONTENT

Supporting Information

The Supporting Information is available free of charge on the ACS Publications website at DOI: 10.1021/acs.jpcb.8b03632.

Histograms for vasopressin; frustration indices for the coiled coil and ubiquitin; frustration indices for RNA 7SK and its mutants; mutations of atomic clusters (PDF)

■ AUTHOR INFORMATION

Corresponding Author

*E-mail: dw34@cam.ac.uk.

ORCID

Konstantin Röder: 0000-0003-2021-9504

David J. Wales: 0000-0002-3555-6645

Notes

The authors declare no competing financial interest.

■ ACKNOWLEDGMENTS

The authors thank Prof. Sir A. Fersht, Prof. P. G. Wolynes, Prof. J. N. Onuchic, J. Joseph, L. Dicks, and S. Niblett for their

DOI: 10.1021/acs.jpcb.8b03632
J. Phys. Chem. B XXXX, XXX, XXX−XXX

comments on the manuscript and the EPSRC for financial support.

REFERENCES

(1) Bryngelson, J. D.; Wolynes, P. G. Spin glasses and the statistical mechanics of protein folding. *Proc. Natl. Acad. Sci. U. S. A.* **1987**, *84*, 7524−7528.
(2) Bryngelson, J. D.; Wolynes, P. G. Intermediates and barrier crossing in a random energy model (with applications to protein folding). *J. Phys. Chem.* **1989**, *93*, 6902−6915.
(3) Leopold, P. E.; Montal, M.; Onuchic, J. N. Protein folding funnels: a kinetic approach to the sequence-structure relationship. *Proc. Natl. Acad. Sci. U. S. A.* **1992**, *89*, 8721−8725.
(4) Bryngelson, J. D.; Onuchic, J. N.; Socci, N. D.; Wolynes, P. G. Funnels, pathways, and the energy landscape of protein folding: A synthesis. *Proteins: Struct., Funct., Genet.* **1995**, *21*, 167−195.
(5) Onuchic, J. N.; Wolynes, P. G. Theory of protein folding. *Curr. Opin. Struct. Biol.* **2004**, *14*, 70−75.
(6) Ferreiro, D. U.; Komives, E. A.; Wolynes, P. G. Frustration in biomolecules. *Q. Rev. Biophys.* **2014**, *47*, 285−363.
(7) Morcos, F.; Schafer, N. P.; Cheng, R. R.; Onuchic, J. N.; Wolynes, P. G. Coevolutionary information, protein folding landscapes, and the thermodynamics of natural selection. *Proc. Natl. Acad. Sci. U. S. A.* **2014**, *111*, 12408−12413.
(8) Nelson, E. D.; Onuchic, J. N. Proposed mechanism for stability of proteins to evolutionary mutations. *Proc. Natl. Acad. Sci. U. S. A.* **1998**, *95*, 10682−10686.
(9) Wolynes, P. G. Evolution, energy landscapes and the paradoxes of protein folding. *Biochimie* **2015**, *119*, 218−230.
(10) Matouschek, A.; Kellis, J. T.; Serrano, L.; Fersht, A. R. Mapping the transition state and pathway of protein folding by protein engineering. *Nature* **1989**, *340*, 122.
(11) Fersht, A. *Structure and mechanism in protein science*; Freeman: New York, 1999.
(12) Ball, K. D.; Berry, R. S.; Kunz, R. E.; Li, F.-Y.; Proykova, A.; Wales, D. J. From topographies to dynamics on multidimensional potential energy surfaces of atomic clusters. *Science* **1996**, *271*, 963−966.
(13) Wales, D. J.; Miller, M. A.; Walsh, T. R. Archetypal energy landscapes. *Nature* **1998**, *394*, 758−760.
(14) Ferreiro, D. U.; Hegler, J. A.; Komives, E. A.; Wolynes, P. G. On the role of frustration in the energy landscapes of allosteric proteins. *Proc. Natl. Acad. Sci. U. S. A.* **2011**, *108*, 3499−503.
(15) Kouza, M.; Hansmann, U. H. E. Folding simulations of the A and B domains of protein G. *J. Phys. Chem. B* **2012**, *116*, 6645−6653.
(16) Joseph, J. A.; Röder, K.; Chakraborty, D.; Mantell, R. G.; Wales, D. J. Exploring biomolecular energy landscapes. *Chem. Commun.* **2017**, *53*, 6974−6988.
(17) Hegler, J. A.; Weinkam, P.; Wolynes, P. G. The spectrum of biomolecular states and motions. *HFSP J.* **2008**, *2*, 307−313.
(18) Whitford, P. C.; Onuchic, J. N.; Wolynes, P. G. Energy landscape along an enzymatic reaction trajectory: Hinges or cracks? *HFSP J.* **2008**, *2*, 61−64.
(19) Wales, D. J. Discrete path sampling. *Mol. Phys.* **2002**, *100*, 3285−3305.
(20) Wales, D. J. Some further applications of discrete path sampling to cluster isomerization. *Mol. Phys.* **2004**, *102*, 891−908.
(21) Noé, F.; Fischer, S. Transition networks for modeling the kinetics of conformational change in macromolecules. *Curr. Opin. Struct. Biol.* **2008**, *18*, 154−162.
(22) Wales, D. J. Energy landscapes: some new horizons. *Curr. Opin. Struct. Biol.* **2010**, *20*, 3−10.
(23) Trygubenko, S. A.; Wales, D. J. A doubly nudged elastic band method for finding transition states. *J. Chem. Phys.* **2004**, *120*, 2082−2094.
(24) Henkelman, G.; Jónsson, H. A dimer method for finding saddle points on high dimensional potential surfaces using only first derivatives. *J. Chem. Phys.* **1999**, *111*, 7010−7022.
(25) Henkelman, G.; Uberuaga, B. P.; Jónsson, H. A climbing image nudged elastic band method for finding saddle points and minimum energy paths. *J. Chem. Phys.* **2000**, *113*, 9901−9904.
(26) Munro, L. J.; Wales, D. J. Defect migration in crystalline silicon. *Phys. Rev. B: Condens. Matter Mater. Phys.* **1999**, *59*, 3969−3980.
(27) Maier, J. A.; Martinez, C.; Kasavajhala, L.; Wickstrom, L.; Hauser, K. E.; Simmerling, C. ff14SB: Improving the accuracy of protein side chain and backbone parameters from ff99SB. *J. Chem. Theory Comput.* **2015**, *11*, 3696−3713.
(28) Onufriev, A.; Bashford, D.; Case, D. A. Modification of the generalized Born model suitable for macromolecules. *J. Phys. Chem. B* **2000**, *104*, 3712−3720.
(29) Onufriev, A.; Bashford, D.; Case, D. A. Exploring protein native states and large-scale conformational changes with a modified generalized born model. *Proteins: Struct., Funct., Genet.* **2004**, *55*, 383−394.
(30) Srinivasan, J.; Trevathan, M. W.; Beroza, P.; Case, D. A. Application of a pairwise generalized Born model to proteins and nucleic acids: inclusion of salt effects. *Theor. Chem. Acc.* **1999**, *101*, 426−434.
(31) Li, Z.; Scheraga, H. A. Monte Carlo-minimization approach to the multiple-minima problem in protein folding. *Proc. Natl. Acad. Sci. U. S. A.* **1987**, *84*, 6611−6615.
(32) Li, Z.; Scheraga, H. A. Structure and free energy of complex thermodynamic systems. *J. Mol. Struct.: THEOCHEM* **1988**, *179*, 333.
(33) Wales, D. J.; Doye, J. P. K. Global optimization by basin-hopping and the lowest energy structures of Lennard-Jones clusters containing up to 110 atoms. *J. Phys. Chem. A* **1997**, *101*, 5111−5116.
(34) Becker, O. M.; Karplus, M. The topology of multidimensional potential energy surfaces: Theory and application to peptide structure and kinetics. *J. Chem. Phys.* **1997**, *106*, 1495−1517.
(35) de Souza, V. K.; Stevenson, J. D.; Niblett, S. P.; Farrell, J. D.; Wales, D. J. Defining and quantifying frustration in the energy landscape: Applications to atomic and molecular clusters, biomolecules, jammed and glassy systems. *J. Chem. Phys.* **2017**, *146*, 124103.
(36) Yadav, M. K.; Leman, L. J.; Price, D. J.; Brooks, C. L.; Stout, C. D.; Ghadiri, M. R. Coiled coils at the edge of configurational heterogeneity. Structural analyses of parallel and antiparallel homotetrameric coiled coils reveal configurational sensitivity to a single solvent-exposed amino acid substitution. *Biochemistry* **2006**, *45*, 4463−4473.
(37) Röder, K.; Wales, D. J. Transforming the energy landscape of a coiled-coil peptide via point mutations. *J. Chem. Theory Comput.* **2017**, *13*, 1468−1477.
(38) Grigoryan, G.; Keating, A. Structural specificity in coiled-coil interactions. *Curr. Opin. Struct. Biol.* **2008**, *18*, 477−483.
(39) Su, L.; Cukier, R. I. Hamiltonian replica exchange method studies of a leucine zipper dimer. *J. Phys. Chem. B* **2009**, *113*, 9595−9605.
(40) Rämisch, S.; Lizatović, R.; André, I. Exploring alternate states and oligomerization preferences of coiled-coils by de novo structure modeling. *Proteins: Struct., Funct., Genet.* **2015**, *83*, 235−247.
(41) Alber, T. How GCN4 binds DNA. *Curr. Biol.* **1993**, *3*, 182−184.
(42) Harbury, P. B.; Zhang, T.; Kim, P. S.; Alber, T. A switch between two-, three-, and four-stranded coiled coils in GCN4 leucine zipper mutants. *Science* **1993**, *262*, 1401−1407.
(43) Gonzalez, L.; Brown, R. A.; Richardson, D.; Alber, T. Crystal structures of a single coiled-coil peptide in two oligomeric states reveal the basis for structural polymorphism. *Nat. Struct. Biol.* **1996**, *3*, 1002−1010.
(44) Levy, Y.; Cho, S. S.; Shen, T.; Onuchic, J. N.; Wolynes, P. G. Symmetry and frustration in protein energy landscapes: A near degeneracy resolves the Rop dimer-folding mystery. *Proc. Natl. Acad. Sci. U. S. A.* **2005**, *102*, 2373−2378.
(45) Gambin, Y.; Schug, A.; Lemke, E. A.; Lavinder, J. J.; Ferreon, A. C. M.; Magliery, T. J.; Onuchic, J. N.; Deniz, A. A. Direct single-molecule observation of a protein living in two opposed native structures. *Proc. Natl. Acad. Sci. U. S. A.* **2009**, *106*, 10153−10158.

DOI: 10.1021/acs.jpcb.8b03632
J. Phys. Chem. B XXXX, XXX, XXX−XXX

(46) Onuchic, J. N.; Wolynes, P. G. Theory of protein folding: The energy landscape perspective. *Annu. Rev. Phys. Chem.* **1997**, *48*, 545−600.
(47) Chebaro, Y.; Ballard, A. J.; Chakraborty, D.; Wales, D. J. Intrinsically disordered energy landscapes. *Sci. Rep.* **2015**, *5*, 10386.
(48) Yedvabny, E.; Nerenberg, P. S.; So, C.; Head-Gordon, T. Disordered structural ensembles of vasopressin and oxytocin and their mutants. *J. Phys. Chem. B* **2015**, *119*, 896−905.
(49) Walter, R.; Yamanaka, T.; Sakakibarat, S. A neurohypophyseal hormone analog with selective oxytocin-like activities and resistance to enzymatic inactivation: An approach to the design of peptide drugs. *Proc. Natl. Acad. Sci. U. S. A.* **1974**, *71*, 1901−1905.
(50) Willcutts, M. D.; Felner, E.; White, P. C. Autosomal recessive familial neurohypophyseal diabetes insipidus with continued secretion of mutant weakly active vasopressin. *Hum. Mol. Genet.* **1999**, *8*, 1303−1307.
(51) Rittig, S.; Siggaard, C.; Ozata, M.; Yetkin, I.; Gregersen, N.; Pedersen, E. B.; Robertson, G. L. Autosomal dominant neurohypophyseal diabetes insipidus due to substitution of histidine for tyrosine 2 in the vasopressin moiety of the hormone precursor. *J. Clin. Endocrinol. Metab.* **2002**, *87*, 3351−3355.
(52) Gladkova, C.; Schubert, A. F.; Wagstaff, J. L.; Pruneda, J. N.; Freund, S. M. V.; Komander, D. An invisible ubiquitin conformation is required for efficient phosphorylation by PINK1. *EMBO J.* **2017**, *36*, 3555.
(53) Schubert, A. F.; Gladkova, C.; Pardon, E.; Wagstaff, J. L.; Freund, S. M. V.; Steyaert, J.; Maslen, S. L.; Komander, D. Structure of PINK1 in complex with its substrate ubiquitin. *Nature* **2017**, *552*, 51−56.
(54) Dawson, T. M.; Dawson, V. L.; Caputo, V.; Muqit, M. M. K.; Harvey, K.; Gispert, S.; Ali, Z.; Turco, D. D.; Bentivoglio, A. R.; Healy, D. G.; et al. Molecular pathways of neurodegeneration in Parkinson's disease. *Science* **2003**, *302*, 819−22.
(55) Wauer, T.; Swatek, K. N.; Wagstaff, J. L.; Gladkova, C.; Pruneda, J. N.; Michel, M. A.; Gersch, M.; Johnson, C. M.; Freund, S. M. V.; Komander, D. Ubiquitin Ser65 phosphorylation affects ubiquitin structure, chain assembly and hydrolysis. *EMBO J.* **2015**, *34*, 307−25.
(56) Dong, X.; Gong, Z.; Lu, Y.-B.; Liu, K.; Qin, L.-Y.; Ran, M.-L.; Zhang, C.-L.; Liu, Z.; Zhang, W.-P.; Tang, C. Ubiquitin S65 phosphorylation engenders a pH-sensitive conformational switch. *Proc. Natl. Acad. Sci. U. S. A.* **2017**, *114*, 6770−6775.
(57) Craig, P. O.; Ltzer, J.; Weinkam, P.; Hoffman, R. M. B.; Ferreiro, D. U.; Komives, E. A.; Wolynes, P. G. Prediction of Native-State Hydrogen Exchange from Perfectly Funneled Energy Landscapes. *J. Am. Chem. Soc.* **2011**, *133*, 17463−17472.
(58) Barrandon, C.; Spiluttini, B.; Bensaude, O. Non-coding RNAs regulating the transcriptional machinery. *Biol. Cell* **2008**, *100*, 83−95.
(59) Diribarne, G.; Bensaude, O. 7SK RNA, a non-coding RNA regulating P-TEFb, a general transcription factor. *RNA Biol.* **2009**, *6*, 122−128.
(60) Sedore, S. C.; Byers, S. A.; Biglione, S.; Price, J. P.; Maury, W. J.; Price, D. H. Manipulation of P-TEFb control machinery by HIV: recruitment of P-TEFb from the large form by Tat and binding of HEXIM1 to TAR. *Nucleic Acids Res.* **2007**, *35*, 4347−4358.
(61) Michels, A. A.; Nguyen, V. T.; Fraldi, A.; Labas, V.; Edwards, M.; Bonnet, F.; Lania, L.; Bensaude, O. MAQ1 and 7SK RNA interact with CDK9/cyclin T complexes in a transcription-dependent manner. *Mol. Cell. Biol.* **2003**, *23*, 4859−69.
(62) Michels, A. A.; Fraldi, A.; Li, Q.; Adamson, T. E.; Bonnet, F. O.; Nguyen, V. T.; Sedore, S. C.; Price, J. P.; Price, D. H.; Lania, L.; et al. Binding of the 7SK snRNA turns the HEXIM1 protein into a P-TEFb (CDK9/cyclin T) inhibitor. *EMBO J.* **2004**, *23*, 2608−2619.
(63) Martinez-Zapien, D.; Legrand, P.; McEwen, A. G.; Proux, F.; Cragnolini, T.; Pasquali, S.; Dock-Bregeon, A.-C. The crystal structure of the 5′ functional domain of the transcription riboregulator 7SK. *Nucleic Acids Res.* **2017**, *45*, 3568−3579.
(64) Wales, D. J. The energy landscape as a unifying theme in molecular science. *Philos. Trans. R. Soc., A* **2005**, *363*, 357−377.
(65) Eaton, W. A.; Wolynes, P. G. Theory, simulations, and experiments show that proteins fold by multiple pathways. *Proc. Natl. Acad. Sci. U. S. A.* **2017**, *114*, E9759−E9760.
(66) Husic, B. E.; Schebarchov, D.; Wales, D. J. Impurity effects on solid-solid transitions in atomic clusters. *Nanoscale* **2016**, *8*, 18326−18340.

DOI: 10.1021/acs.jpcb.8b03632
J. Phys. Chem. B XXXX, XXX, XXX−XXX